

Surgical Resection for Hepatocellular Carcinoma with Cardiac Cirrhosis after the Fontan Procedure

Yoshitaka Takuma¹, Yuji Fukada¹, Shota Iwadou¹, Hirokazu Miyatake¹, Shuji Uematsu¹, Ryoichi Okamoto¹, Daisuke Sato², Hiroyoshi Matsukawa², Shigehiro Shiozaki², Masahiro Kamada³, Toshiaki Morito⁴ and Yasuyuki Araki¹

Abstract

A 29-year-old woman who underwent the Fontan procedure at 10 years of age had an incidental finding of liver masses on abdominal ultrasonography. Subsequent gadolinium ethoxybenzyl diethylenetriamine pentaacetic acid magnetic resonance imaging showed a 15 mm hypervascular mass with washout in the hepatobiliary phase in liver segment 4 (S4), and an 18 mm hypervascular mass without washout in the hepatobiliary phase in liver segment 2 (S2). The S2 liver mass was pathologically diagnosed to be a regenerative nodule by an ultrasound-guided needle biopsy, and the S4 liver mass was pathologically diagnosed as a poorly differentiated hepatocellular carcinoma after partial hepatectomy.

Key words: hepatocellular carcinoma (HCC), Fontan, cardiac cirrhosis, surgical resection

(Intern Med 55: 3265-3272, 2016)

(DOI: 10.2169/internalmedicine.55.6869)

Introduction

The Fontan procedure is used to separate the systemic and pulmonary circulations in patients with various forms of functionally univentricular hearts. In the Fontan circulation, systemic venous return is sent to the pulmonary arteries without passage through a ventricle. The Fontan procedure can result in various late complications, including central venous hypertension, diminished oxygen delivery, reduced cardiac output, venous thrombosis, and arrhythmia (1, 2). These complications caused by central venous hypertension lead to parenchymal injury, fibrosis, and cirrhosis of the liver (2, 3). Cardiac cirrhosis is a serious late complication of congenital heart disease and can cause hepatocellular carcinoma (HCC) (4, 5). However, the prevalence and risk factors of cirrhotic changes and HCCs have not been clearly identified. Furthermore, non-invasive diagnostic tools for hepatic fibrosis and the management of HCC in patients after undergoing the Fontan procedure have not yet been clearly established.

We herein report a case of HCC with cardiac cirrhosis treated with surgical resection.

Case Report

A 29-year-old woman with a history of a univentricular heart had undergone a Fontan operation 10 years of age. She also had situs inversus. She was followed-up at the department of pediatric cardiology in our hospital, and regularly underwent blood examinations without alpha-fetoprotein (AFP) at 2- or 3-month intervals. The results showed that the transaminase level was within the normal range. On a routine follow-up day, she experienced slight abdominal discomfort and received abdominal ultrasonography (US). She had an incidental finding of liver masses and was referred to our department.

B-mode conventional US showed a 15 mm hypoechoic mass in liver segment 4 (S4) (Fig. 1a), and an 18 mm hyperechoic mass in liver segment 2 (S2) (Fig. 2a). Furthermore, the liver parenchyma had a coarsened appearance consistent with cirrhosis, and ascites and splenomegaly were

¹Department of Internal Medicine, Hiroshima City Hospital, Japan, ²Department of Surgery, Hiroshima City Hospital, Japan, ³Department of Pediatric Cardiology, Hiroshima City Hospital, Japan and ⁴Department of Pathology, Hiroshima City Hospital, Japan

Received for publication November 20, 2015; Accepted for publication January 7, 2016

Correspondence to Dr. Yoshitaka Takuma, takuma@enjoy.ne.jp

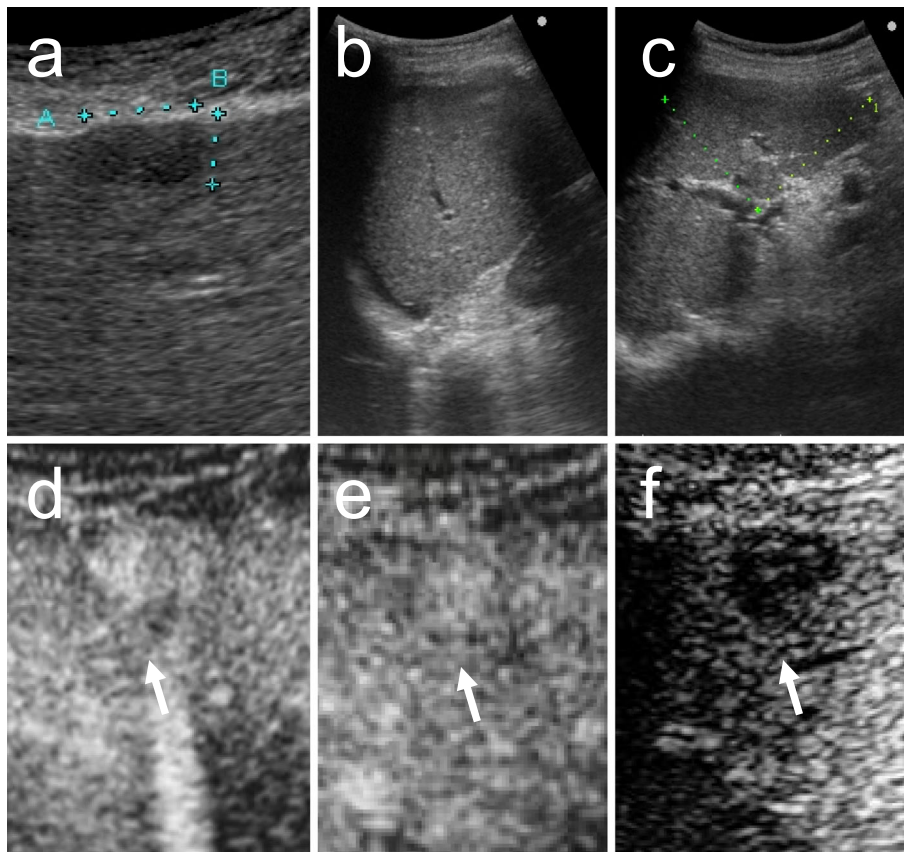


Figure 1. Ultrasonography findings (arrows). B-mode conventional ultrasonography showed a 15 mm hypoechoic mass in liver segment 4 (S4) (a), the liver parenchyma had a coarsened appearance consistent with cirrhosis, and ascites and splenomegaly were observed (b, c). CEUS using Sonazoid showed a homogeneously enhanced mass in the arterial dominant phase (d), a hypoechoic mass relative to the adjacent liver parenchyma during the portal dominant phase (e), and a contrast defect with a clear border in the postvascular phase (f).

observed (Fig. 1b and c).

We next performed contrast-enhanced US (CEUS) using a bolus injection of 0.015 mL/kg Sonazoid (perfluorobutane; Daiichi-Sankyo, Tokyo, Japan). The mass lesion in S4 was homogeneously enhanced in the arterial dominant phase (from 10 to 30 seconds) (Fig. 1d). The lesion became progressively hypoechoic relative to the adjacent liver parenchyma during the portal dominant phase (from 30 to 120 seconds) (Fig. 1e), and provided a contrast defect with a clear border in the postvascular phase (10 minutes later) (Fig. 1f). The mass lesion in S2 was homogeneously enhanced in the arterial dominant phase (Fig. 2b). The lesion became isoechoic mass relative to the adjacent liver parenchyma during the portal dominant phase (Fig. 2c) and provided no defects in the postvascular phase (10 minutes later) (Fig. 2d).

We subsequently performed magnetic resonance imaging (MRI) with conventional T1- and T2-weighted imaging (WI) before and after contrast media administration, including diffusion imaging. The contrast media used was hepatocyte-specific Primovist [gadolinium ethoxybenzyl diethylenetriamine pentaacetic acid (Gd-EOB-DTPA); Bayer Schering Pharma, Berlin, Germany]. There was radiographic evidence

of liver cirrhosis with portal hypertension, including a nodular surface, a coarse texture, ascites, and splenomegaly on MRI (Fig. 3a and b).

This imaging revealed a mass lesion in S4 with a moderately low intensity in T1-WI (Fig. 3c) and moderately high intensity in T2-WI (Fig. 3d). In diffusion imaging, the lesion showed a moderately high intensity (Fig. 3e). In the post-contrast phases, the lesion revealed homogeneous enhancement in the arterial phase at 20 seconds (Fig. 3b and f), and washout in the portal phase at 70 seconds and interstitial phase at 180 seconds. At 20 minutes (hepatobiliary phase) after the contrast uptake the lesion showed washout (Fig. 3g). According to these findings, a final diagnosis of HCC was made. In addition, MRI imaging revealed a mass lesion in S2 with a moderately high intensity in T1-WI (Fig. 4b) and moderately low intensity in T2-WI (Fig. 4c). In diffusion imaging, the lesion showed a moderately low intensity (Fig. 4d). In the postcontrast phases, the lesion revealed a homogeneous enhancement in the arterial phase (Fig. 4a and e), an isoenhancement relative to the adjacent liver parenchyma in the portal and interstitial phases, and a high intensity in the hepatobiliary phase (Fig. 4f).

The laboratory data are given in Table 1. Her liver func-

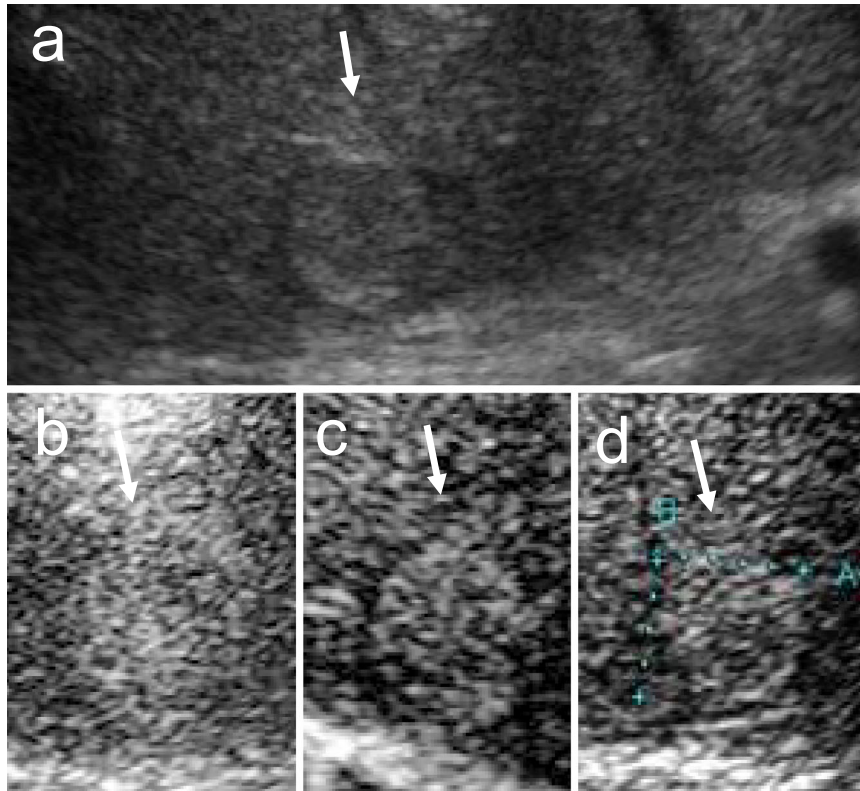


Figure 2. B-mode conventional ultrasonography showed an 18 mm hyperechoic mass in liver segment 2 (S2) (a); and CEUS showed a homogeneously enhanced mass in the arterial dominant phase (b), isoechoic mass relative to the adjacent liver parenchyma during the portal dominant phase (c), and no defects in the postvascular phase (d).

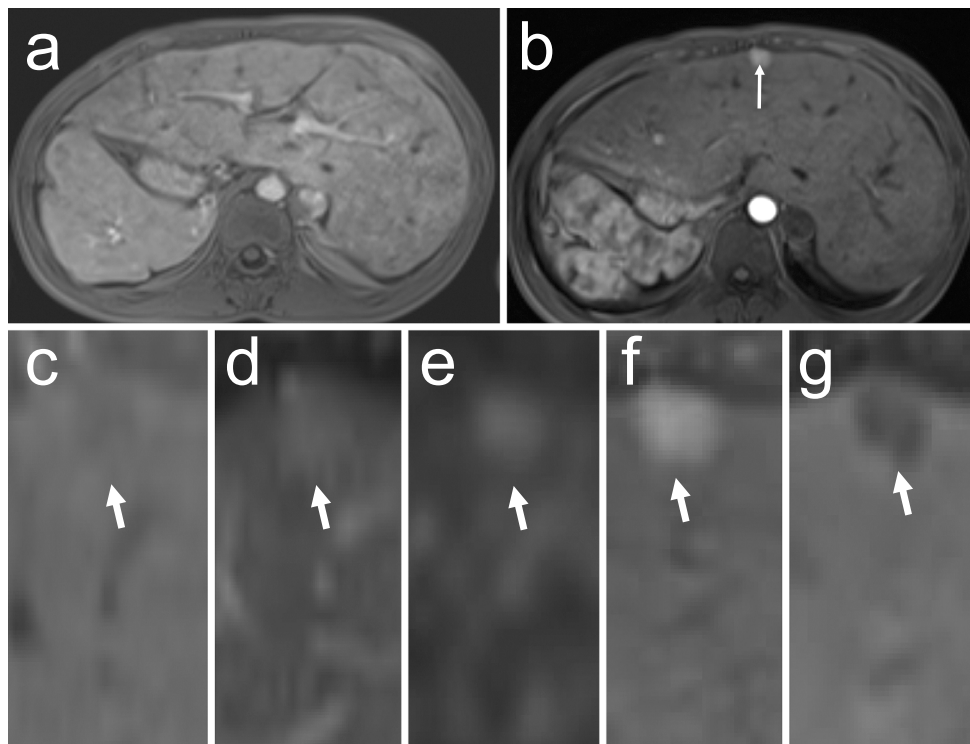


Figure 3. There was radiographic evidence of liver cirrhosis with portal hypertension, including a nodular surface, a coarse texture, ascites, and splenomegaly on MRI (a, b). Gd-EOB-DTPA MRI showed a 15 mm S4 mass with a moderately low intensity in T1-WI (c), moderately high intensity in T2-WI (d), moderately high intensity in diffusion (e), homogeneous arterial enhancement (b, f), and complete washout in the hepatobiliary phase (g).

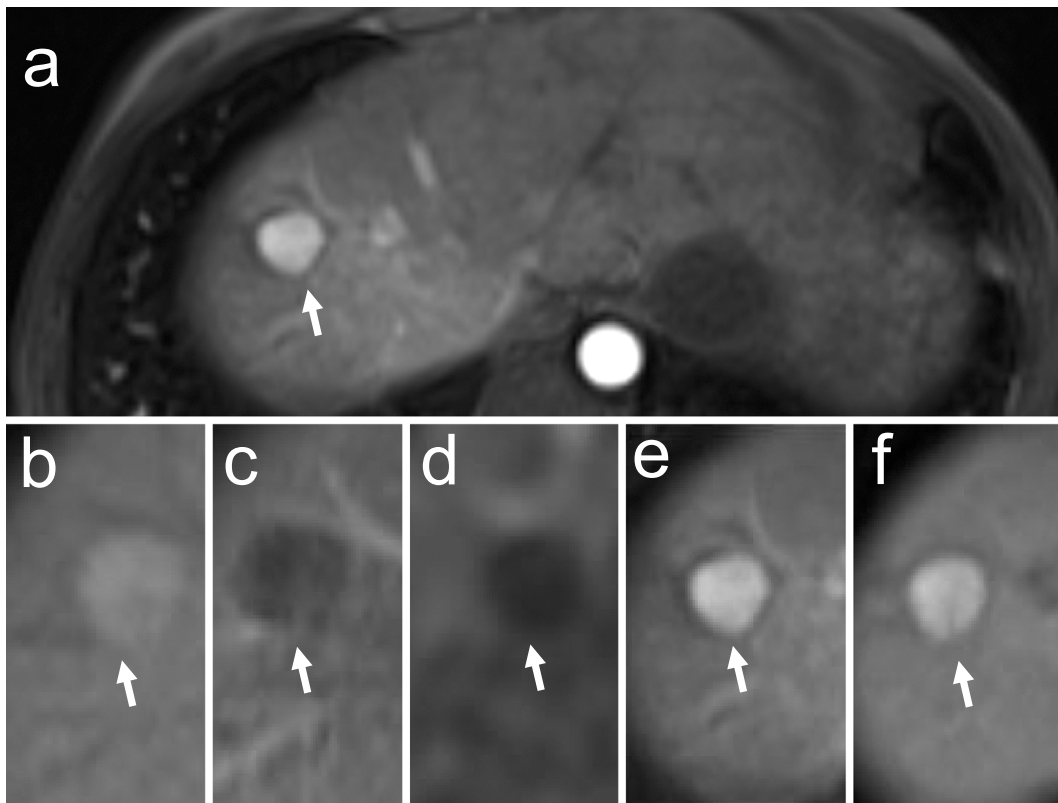


Figure 4. Gd-EOB-DTPA MRI showed an 18 mm S2 mass with a moderately high intensity in T1-WI (b), moderately low intensity in T2-WI (c), moderately low intensity in diffusion (d), homogeneous arterial enhancement (a, e), and high intensity in the hepatobiliary phase (f).

Table 1. Results of Blood Tests.

Hematology		Blood biochemistry		Serology	
WBC	3.0 ×10 ³ /μL	TP	7.7 g/dL	HBsAg	(-)
RBC	494×10 ⁴ /μL	Alb	4.9 g/dL	HBsAb	(-)
Hb	9.5 g/dL	ChE	166 IU/L	HBcAb	(-)
Hct	32.7%	T.Bil	1.0 mg/dL	HCV-Ab	(-)
PLT	12.5×10 ⁴ /μL	D.Bil	0.5 mg/dL	ANA	(-)
		AST	23 IU/L	AMA-M2	(-)
		ALT	13 IU/L	IgG	1,267 mg/dL
		LDH	226 IU/L	IgA	233 mg/dL
Coagulation test		ALP	163 IU/L	IgM	231 mg/dL
PT%	33.1 %	γ-GTP	47 IU/L	AFP	117.1 ng/mL
PT-INR	1.68	ZTT	8.5 KU	AFP-L3	46.8 %
		TTT	4.6 KU	CEA	0.4 ng/mL
		BUN	19mg/dL	CA19-9	5.1 ng/mL
		Cr	0.79mg/dL		
		CRP	0.010 mg/dL		
		hyaluronic acid	53 ng/mL		
		type IV collagen7S	8.5 ng/mL		
		ICG-R15	19.9%		

WBC: white blood cells, RBC: red blood cells, Hb: hemoglobin, Hct: hematocrit, PLT: platelets, PT: prothrombin time, INR: international normalized ratio, TP: total protein, Alb: albumin, ChE: cholinesterase, T.Bil: total bilirubin, D.Bil: direct bilirubin, AST: aspartate aminotransferase, ALT: alanine aminotransferase, LDH: lactate dehydrogenase, ALP: alkaline phosphatase, γ-GTP: γ-glutamyltranspeptidase, ZTT: zinc sulfate turbidity test, TTT: thymol turbidity test, BUN: blood urea nitrogen, Cr: creatinine, CRP: C-reactive protein, ICG-R: indocyanine green retention, HBsAg: hepatitis B surface antigen, HBsAb: hepatitis B surface antibody, HBcAb: hepatitis B core antibody, HCV: hepatitis C virus antibody, ANA: antinuclear antibodies, AMA-M2: anti-mitochondrial M2 antibody, AFP: alpha-fetoprotein, AFP-L3: Lens culinaris agglutinin-reactive fraction of AFP, CEA: carcinoembryonic antigen, CA: carbohydrate antigen

tion was well preserved with the Child-Pugh classification A, and her international normalized ratio was low (the patient was on warfarin for atrial arrhythmia). Other lab findings included a high AFP level [normal less than 40 nan-

ograms/milliliter (ng/mL)], high Lens culinaris agglutinin-reactive fraction of AFP (AFP-L3) (normal less than 10%), low platelet count (normal greater than 150,000/microliter), high hyaluronic acid (normal less than 50 ng/mL), and high

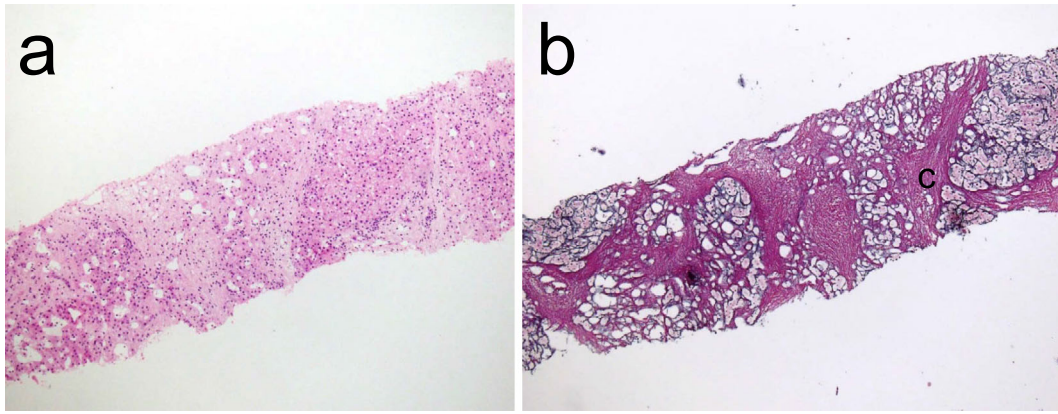


Figure 5. A histological specimen was obtained by an ultrasound-guided needle biopsy of the S2 lesion. Microscopic histological findings revealed bridging fibrosis in the liver section. The parenchymal cells did not display cellular or structural atypia [Hematoxylin and Eosin staining (a), and silver impregnation (b) with a low-power field]. The liver mass in S2 was pathologically diagnosed as a regenerative nodule.

type IV collagen 7S (normal less than 6.0 ng/mL). An echocardiogram demonstrated a normal ventricular function and no obstruction in the Fontan circuit. The patient had no other significant medical problems and no other risk factors for cirrhosis, as she expressed negativity for viral and autoimmune markers, no alcoholic consumption, no hepatotoxic drugs (such as amiodarone), and no metabolic factors such as diabetes mellitus, obesity (her body mass index was 17.7), or fatty liver in US. Following the reversal of her warfarin therapy, an ultrasound-guided needle biopsy of the S2 lesion was performed. Histological findings revealed that bridging fibrosis in the liver section, and the parenchymal cells did not display cellular or structural atypia (Fig. 5). The liver mass in S2 was pathologically diagnosed to be a regenerative nodule.

The patient underwent a curative operation, involving partial hepatectomy of S4 in the liver. Macroscopically, sections of the specimen revealed a yellowish-white encapsulated solid tumor measuring 15 mm in size (Fig. 6a).

The growth pattern of the liver tumor showed expansive growth with extracapsular invasions (Fig. 6b). The tumor cells had an increased nuclear/cytoplasmic ratio, polymorphic, and chromatin-rich nuclei, and the pathological diagnosis was poorly differentiated HCC (Fig. 6c). The non-cancerous area of the resected specimen revealed that bridging fibrosis was observed without fat deposition, and the patient was diagnosed with liver cirrhosis (Fig. 7a). Fibrosis was observed in both the portal and pericellular areas, the sinusoidal structure was maintained, but no significant inflammation was observed (Fig. 7b and c).

After discharge from the hospital, the patient was followed-up at 3-month intervals.

At the 1-year follow-up, her AFP level was 2.7 ng/mL, AFP-L3 was less than 0.5%, and the tumor markers remained normal. Furthermore, US and MRI showed no evidence of HCC recurrence.

Discussion

In the present case, there were no known etiological factors such as hepatitis viral infection, alcoholic liver disease, autoimmune liver diseases, autoimmune hepatitis, primary biliary cirrhosis, metabolic liver diseases [such as non-alcoholic steatohepatitis (NASH)], or medication with hepatotoxic drugs (such as amiodarone). Moreover, significant hepatic inflammation or fat deposition was not seen as a result of processes such as hepatitis viral infection or NASH. On histology in the present case, hepatic sinusoidal fibrosis extending from centrilobular areas toward the portal tract without inflammation were observed. Schwarz et al. discussed that hepatic fibrosis after the Fontan procedure was a mixed disease that affects both the portal and centrilobular areas in liver biopsy and autopsy specimens (6, 7). Sinusoidal fibrosis is believed to result from an increase in central venous pressure transmitted to hepatic cells that surround the central veins, because the extent of cirrhosis is strongly correlated with elevated hepatic venous pressures and a low cardiac index in patients after undergoing the Fontan procedure (8). After Fontan palliation, a significant liver disease can result in central venous congestion and hypoxia resulting from a low cardiac output, however, little is known regarding fibrogenic mechanisms independent of the inflammation-mediated pathway in congestive liver disease (CLD). In CLD, mechanotransduction associated with stretching and compression of hepatic stellate cells may be a potent inducer of hepatic fibrosis (9, 10). Using a newly characterized murine CLD model, sinusoidal thrombosis and mechanical stretching of adjacent hepatic stellate cells caused by sinusoidal dilatation was shown to induce the release of fibronectin by hepatic stellate cells, and both fibrin and stretching stimulated fibronectin fibril assembly through a $\beta 1$ -integrin and actin-dependent mechanism (11).

In addition, hepatic complications after the Fontan proce-

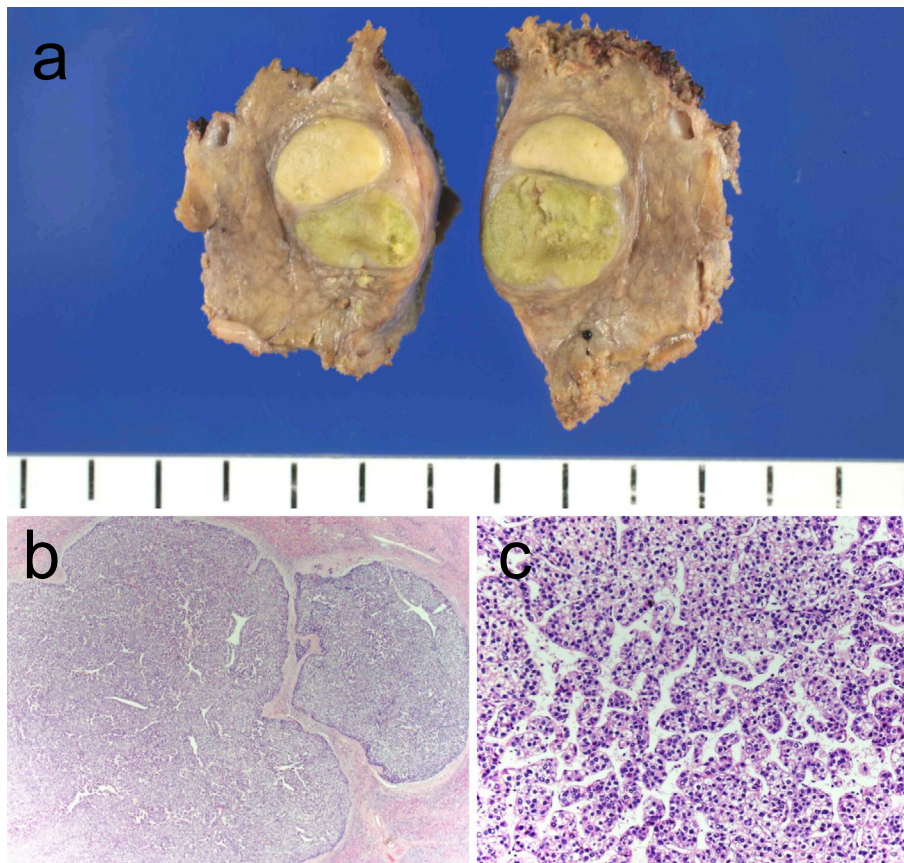


Figure 6. A macroscopic appearance of the resected S4 specimen revealed a yellowish-white encapsulated solid tumor measuring 15 mm in size (a). Microscopically, the growth pattern of the S4 liver tumor showed expansive growth with extracapsular invasions [b, Hematoxylin and Eosin (H&E) staining with a low-power field]. Tumor cells had an increased nuclear/cytoplasmic ratio, polymorphic, and chromatin-rich nuclei, and the pathological diagnosis was poorly differentiated HCC (c, H&E staining with a high-power field).

ture are associated with the duration of follow-up (8, 12). Progression to cirrhosis may even be observed within 10 years after the initial Fontan procedure (13). In 34 patients with a median follow-up of 11.5 years after the Fontan procedure, 30% experienced abnormal transaminases, 61% abnormal γ -GTP, 32% abnormal bilirubin, and 58% coagulopathy (14). As compared to a duration of 0-5 years, the odds ratio of hepatic complications was 4.4 for a post-Fontan duration of 11-15 years and 9.0 for a duration of 16-20 years, respectively (12).

Liver cirrhosis is a potential prerequisite for HCC, however, the prevalence and progression of cirrhotic changes in the Fontan population have not been clearly identified. Non-invasive diagnostic tools for hepatic fibrosis are needed, because a liver biopsy, the golden standard for diagnosing liver cirrhosis, is difficult to perform in Fontan patients due to prophylactic anticoagulation. Similar to the present case, a radiological assessment of liver fibrosis using various methods such as US, CT, or MRI may be useful.

There are several reports of HCC in patients with CLD following the Fontan procedure.

As shown in Table 2, a recent PubMed search identified 12 cases of HCCs among published reports. The publica-

tions described the use of surgical resection, transcatheter arterial chemoembolization, radioembolization, local ablation, or sorafenib therapy (15-22). In previous reports, two patients were treated with surgical resection (20, 21). For early stage HCC, surgical resection provides curative treatment with a long-time survival, however, hepatectomy is rarely performed following the Fontan procedure because it is difficult to detect early stage HCCs. Although the present patient did not receive periodic surveillance for HCC, such as US and AFP, it is fortunate that early stage HCC was incidentally detected. HCC detected after the onset of symptoms has a poor prognosis (5-year survival rate of 0-10%). In contrast, early stage HCCs detected by surveillance can be cured with both surgical resection and liver transplantation (5-year disease-free survival rate >50%) (23).

Thus, surveillance for HCC may be necessary in patients with CLD who undergo the Fontan procedure because cirrhosis is a high-risk factor for HCC. However, the screening interval for liver disease after the Fontan procedure has not yet been established. Surveillance is based on an ultrasound examination, and the recommended screening interval is 6 months according to the American Association for the Study of Liver Diseases (AASLD) practice guidelines on the man-

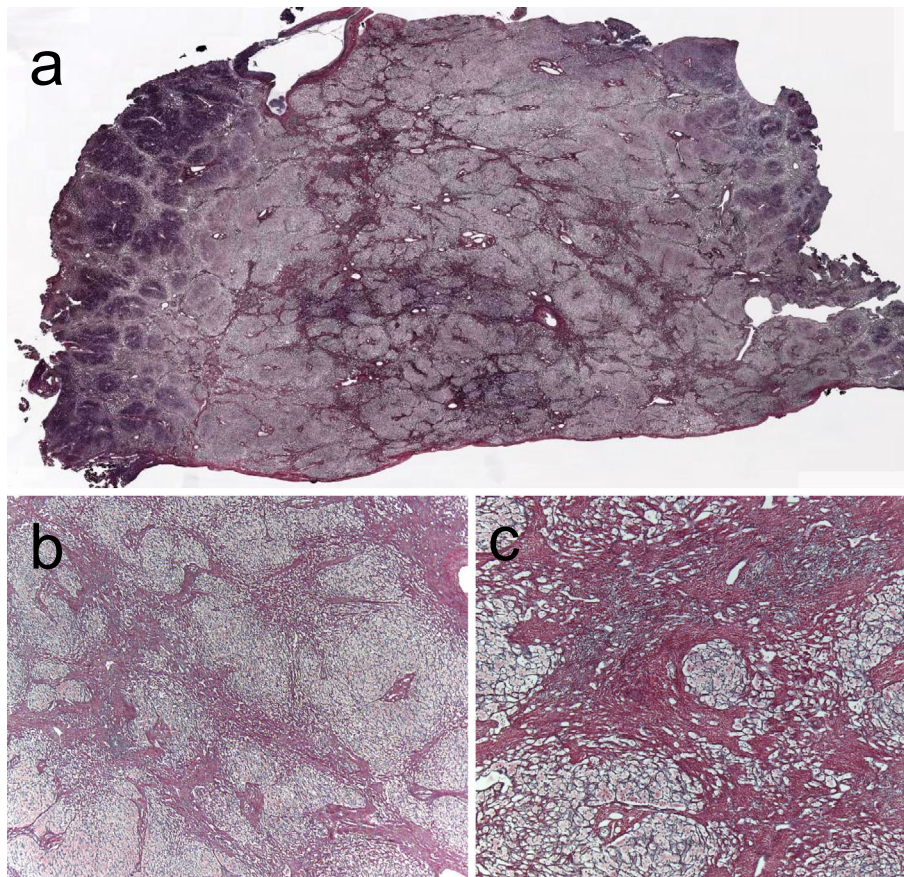


Figure 7. The non-cancerous area of the resected specimen revealed bridging fibrosis without fat deposition, and the patient was diagnosed with liver cirrhosis [silver impregnation (a)]. Fibrosis was observed in both the portal and pericellular areas, the sinusoidal structure was maintained, and significant inflammation was not seen [silver impregnation (b, c) with a high-power field].

Table 2. Reported Cases of Hepatocellular Carcinoma after Fontan Procedure.

Reference	No. of cases	Age(y)	Sex	AFP (ng/mL)	Size (mm)	Treatment	Outcome
15	1	24	M	ND	40	ND	Died
16	2	27	F	162.7	22.1	Systemic chemo	Died
		28	F	788	40	Sorafenib	Died
17	4	32	F	700	40	TACE	Alive
		24	M	5,000	ND	ND	Died
		33	M	630	ND	Radioembolization	Died
		42	F	106	ND	TACE	Alive
18	1	51	M	ND	10	Local ablation	Alive
19	1	19	F	ND	ND	Sorafenib	Died
20	1	23	F	ND	148	Surgical resection	Alive
21	1	32	M	13	40	Surgical resection	Alive
22	1	15	M	2	ND	TAE	Died
Our case	1	29	F	117.1	15	Surgical resection	Alive

F: female, M: male, ND: not described, TACE: transarterial chemoembolization, TAE: transarterial embolization

agement of HCC (24). In addition, the AFP level in the present case was high. In Japan (25), all patients with high-risk factors for HCC are advised to undergo periodic surveillance with US and laboratory work ups, including AFP and protein induced by vitamin K absence or antagonists-II (PIVKA-II), every 6 months. However, similar to the present case, PIVKA-II is not useful in most patients after the Fontan procedure because prophylactic antiplatelet with anticoagulation therapies, such as warfarin administration, are necessary to prevent thromboembolic events, which are one of

the major causes of morbidity and mortality (26). Following the Fontan procedure, patients face a risk of HCC and require a lifelong follow-up with not only a pediatric cardiologist, but also a hepatologist experienced in the care of patients with liver cirrhosis.

We herein described a patient with HCC who was able to safely undergo liver resection following the Fontan procedure under a preserved cardiac and hepatic function.

The authors state that they have no Conflict of Interest (COI).

References

1. Kendall TJ, Stedman B, Hacking N, et al. Hepatic fibrosis and cirrhosis in the Fontan circulation: a detailed morphological study. *J Clin Pathol* **61**: 504-508, 2008.
2. Wanless IR, Liu JJ, Butany J. Role of thrombosis in the pathogenesis of congestive hepatic fibrosis (cardiac cirrhosis). *Hepatology* **21**: 1232-1237, 1995.
3. Kaulitz R, Luhmer I, Bergmann F, Rodeck B, Hausdorf G. Sequelae after modified Fontan operation: postoperative haemodynamic data and organ function. *Heart* **78**: 154-159, 1997.
4. Warnes CA, Williams RG, Bashore TM, et al. ACC/AHA 2008 guidelines for the management of adults with congenital heart disease: a report of the American College of Cardiology/American Heart Association Task Force on Practice Guidelines (Writing Committee to Develop Guidelines on the Management of Adults With Congenital Heart Disease). Developed in Collaboration With the American Society of Echocardiography, Heart Rhythm Society, International Society for Adult Congenital Heart Disease, Society for Cardiovascular Angiography and Interventions, and Society of Thoracic Surgeons. *J Am Coll Cardiol* **52**: e143-e263, 2008.
5. Asrani SK, Asrani NS, Freese DK, et al. Congenital heart disease and the liver. *Hepatology* **56**: 1160-1169, 2012.
6. Schwartz MC, Sullivan L, Cohen MS, et al. Hepatic pathology may develop before the Fontan operation in children with functional single ventricle: an autopsy study. *J Thorac Cardiovasc Surg* **143**: 904-909, 2012.
7. Schwartz MC, Sullivan LM, Glatz AC, et al. Portal and sinusoidal fibrosis are common on liver biopsy after Fontan surgery. *Pediatr Cardiol* **34**: 135-142, 2013.
8. Kiesewetter CH, Sheron N, Vettukattill JJ, et al. Hepatic changes in the failing Fontan circulation. *Heart* **93**: 579-584, 2007.
9. Rockey DC. Current and future anti-fibrotic therapies for chronic liver disease. *Clin Liver Dis* **12**: 939-962, xi, 2008.
10. Goto T, Mikami KI, Miura K, et al. Mechanical stretch induces matrix metalloproteinase 1 production in human hepatic stellate cells. *Pathophysiology* **11**: 153-158, 2004.
11. Simonetto DA, Yang HY, Yin M, et al. Chronic passive venous congestion drives hepatic fibrogenesis via sinusoidal thrombosis and mechanical forces. *Hepatology* **61**: 648-659, 2015.
12. Baek JS, Bae EJ, Ko JS, et al. Late hepatic complications after Fontan operation; non-invasive markers of hepatic fibrosis and risk factors. *Heart* **96**: 1750-1755, 2010.
13. Pike NA, Evangelista LS, Doering LV, Koniak-Griffin D, Lewis AB, Child JS. Clinical profile of the adolescent/adult Fontan survivor. *Congenit Heart Dis* **6**: 9-17, 2011.
14. Camposilvan S, Milanese O, Stellin G, Pettenazzo A, Zancan L, D'Antiga L. Liver and cardiac function in the long term after Fontan operation. *Ann Thorac Surg* **86**: 177-182, 2008.
15. Ghaferi AA, Hutchins GM. Progression of liver pathology in patients undergoing the Fontan procedure: Chronic passive congestion, cardiac cirrhosis, hepatic adenoma, and hepatocellular carcinoma. *J Thorac Cardiovasc Surg* **129**: 1348-1352, 2005.
16. Saliba T, Dorkhom S, O'Reilly EM, Ludwig E, Gansukh B, Abou-Alfa GK. Hepatocellular carcinoma in two patients with cardiac cirrhosis. *Eur J Gastroenterol Hepatol* **22**: 889-891, 2010.
17. Asrani SK, Warnes CA, Kamath PS. Hepatocellular carcinoma after the Fontan procedure. *N Engl J Med* **368**: 1756-1757, 2013.
18. Elder RW, Parekh S, Book WM. More on hepatocellular carcinoma after the Fontan procedure. *N Engl J Med* **369**: 490, 2013.
19. Rajoriya N, Clift P, Thorne S, Hirschfield GM, Ferguson JW. A liver mass post-Fontan operation. *QJM* **107**: 571-572, 2014.
20. Weyker PD, Allen-John Webb C, Emond JC, Brentjens TE, Johnston TA. Anesthetic implications of extended right hepatectomy in a patient with fontan physiology. *A A Case Rep* **2**: 99-101, 2014.
21. Kwon S, Scovel L, Yeh M, et al. Surgical management of hepatocellular carcinoma after Fontan procedure. *J Gastrointest Oncol* **6**: E55-E60, 2015.
22. Yamada K, Shinmoto H, Kawamura Y, et al. Transarterial embolization for pediatric hepatocellular carcinoma with cardiac cirrhosis. *Pediatr Int* **57**: 766-770, 2015.
23. Llovet JM, Burroughs A, Bruix J. Hepatocellular carcinoma. *Lancet* **362**: 1907-1917, 2003.
24. Bruix J, Sherman M; American Association for the Study of Liver D. Management of hepatocellular carcinoma: an update. *Hepatology* **53**: 1020-1022, 2011.
25. Kudo M, Izumi N, Kokudo N, et al. Management of hepatocellular carcinoma in Japan: Consensus-Based Clinical Practice Guidelines proposed by the Japan Society of Hepatology (JSH) 2010 updated version. *Dig Dis* **29**: 339-364, 2011.
26. Monagle P, Karl TR. Thromboembolic problems after the Fontan operation. *Semin Thorac Cardiovasc Surg Pediatr Card Surg Annu* **5**: 36-47, 2002.

The Internal Medicine is an Open Access article distributed under the Creative Commons Attribution-NonCommercial-NoDerivatives 4.0 International License. To view the details of this license, please visit (<https://creativecommons.org/licenses/by-nc-nd/4.0/>).